

Hierarchical Explanations for Video Action Recognition

Sadaf Gulshad, Teng Long, Nanne van Noord
University of Amsterdam

{s.gulshad, t.long, n.j.e.vannoord}@uva.nl

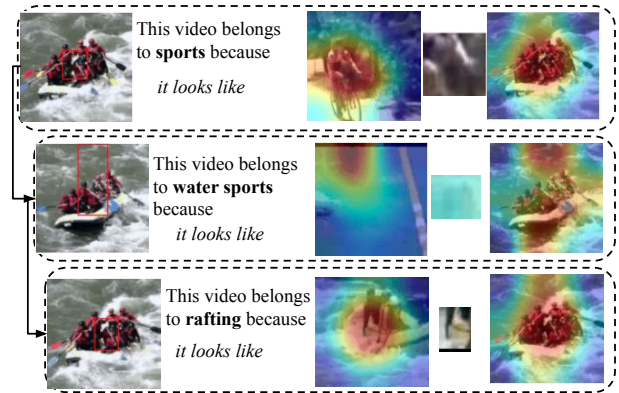
Abstract

We propose *Hierarchical ProtoPNet*: an interpretable network that explains its reasoning process by considering the hierarchical relationship between classes. Different from previous methods that explain their reasoning process by dissecting the input image and finding the prototypical parts responsible for the classification, we propose to explain the reasoning process for video action classification by dissecting the input video frames on multiple levels of the class hierarchy. The explanations leverage the hierarchy to deal with uncertainty, akin to human reasoning: When we observe water and human activity, but no definitive action it can be recognized as the water sports parent class. Only after observing a person swimming can we definitively refine it to the swimming action. Experiments on ActivityNet and UCF-101 show performance improvements while providing multi-level explanations. Our implementation is available at <https://github.com/sadafgulshad1/Hierarchical-ProtoPNet>

1. Introduction

When describing the world around us we may do so at different levels of granularity, depending on the information available or the level of detail we intend to convey. For instance, a video might open with a shot of a cheering crowd, allowing us to recognize it as a *sports event*, as the camera then pans to the river we can deduce that it is a *water sports event*. However, only when the raft comes into the frame can we determine that it concerns *rafting*. Nonetheless, in our description of this video, we may still only refer to it as a sports or water sports event. Our reasoning and description processes build on the hierarchical relation between classes, allowing for navigation between generic and specific. In this work, we implement this process for video action recognition by learning hierarchical prototypes that we leverage for improved classification performance and explanations at multiple levels of granularity.

Despite the remarkable performance of neural networks for video understanding tasks [4, 6, 14, 17, 34, 37, 38, 50] it is still hard to explain the decisions of these networks, which



Leftmost: Parts in the original video that are highly activated by the prototype. Second column: Training videos where prototypes come from. Third column: Prototypes. Rightmost: Saliency map in the original video that are highly activated by the prototype.

Figure 1. **Multi-level Explanations.** Multi-level explanation for a video of rafting with Hierarchical ProtoPNet, showing the explanations at grandparent, parent, and class level.

is of utmost importance for practical application. This necessity has led to a growing stream of research that focuses on making models interpretable besides performing accurately [13, 15, 19, 23, 45]. A promising line of explainability methods are the case-based reasoning models [7, 9, 21], which focus on learning prototypes during the training and making predictions based on the learned prototypes while inference. This enables this look like that type of explanation. However, previous case-based reasoning works are limited to 2D images and models. Moreover, they provide a single level of explanations and in case of uncertainty, the explanations can be as bad as arbitrary, as each explanation is considered equally apart. In this work, we focus on capturing the hierarchical relations between actions to provide multi-level explanations for videos. A challenge for models with built-in explainability, such as case-based reasoning models, is that it introduces an accuracy-explainability trade-off, where explainability comes at the cost of accuracy. With this paper, we aim to introduce a model with built-in explainability, whilst being less affected by this trade-off. To achieve this goal we are inspired by recent

works on learning hyperbolic embedding spaces rather than euclidean for natural language processing [8, 44] and computer vision tasks [1, 12, 26]. These works have demonstrated that it is beneficial for performance to have the embedding space be guided by hierarchical prior knowledge, which we believe will also benefit explainability. This belief is guided by the similarity between human intuition and the representation of categories in the hyperbolic space.

The main contributions of our paper are: 1) We propose Hierarchical ProtoPNet, a case-based reasoning model for interpreting video action recognition. 2) We demonstrate that while other interpretable models fail to provide explanations in the presence of uncertainty or lack of information our Hierarchical ProtoPNet can overcome these challenges by providing multi-level explanations i.e., at class, parent, or grandparent level. 3) We perform a benchmark and show that our Hierarchical ProtoPNet outperforms its non-hierarchical counterpart.

2. Related Work

2.1. Interpretations for Videos

Interpretations for neural networks can be broadly classified into two categories: 1) fitting explanations to the decisions of the network after it has been trained i.e. *posthoc* [13, 15, 19, 27, 35], 2) building explanation mechanism inherent in the network i.e. *built-in* explanations. [23, 24, 45, 46]. In this work, we focus on learning semantic representations which are used for classification during training rather than explaining a black box network posthoc.

A great deal of previous work has focused on video action recognition, detection, segmentation and more [4, 6, 14, 17, 34, 37, 38, 50], however, most of these works focus on designing black box models for specific tasks. They do not explain why a certain decision is made by the model. Moreover, most of the research in the visual explanations domain focuses on images. Only a few works focus on the interpretation of these networks for videos [2, 16, 23, 41, 42], and it is not possible to directly apply image-based explanation methods to videos due to an extra time dimension in videos.

[16] and [2] focus on visualizing spatio-temporal attention in RNNs, CNNs are used only to extract features. Inspired by class activation maps (CAM) [54] for images [42] extended it for videos by finding both regions and frames responsible for classification. [23] utilized perturbations to extract the most informative parts of the inputs responsible for the outputs. Both [23, 42] are posthoc methods, which means they do not use explanations during prediction therefore they might not be faithful to what the network computes [9]. [41] introduced class feature pyramids, a method that traverses through the whole network and searches for the kernels at different depths of the network responsible for classification, therefore this method is computationally

expensive. In contrast, we enable built-in multi-level explanations that do not add any computational complexity.

In this paper, we enable multi-level explanations for videos by learning hierarchical prototypes for each class and tracing them back to input videos.

2.2. Prototype-based Interpretations

In machine learning the term “prototype” is used in various contexts, in zero-shot learning [22, 51–53] and few-shot learning [32, 39] prototypes are points in the embedding space representing a single class and the distance from these prototypes is used during classification. However, in our work prototypes are closer to the samples in the training set, and multiple prototypes are used to represent each class. They are optimized to resemble the training set in order to provide visual explanations.

The idea to provide built-in explanations with prototypes was first explored in [21], where the authors introduced a prototype layer in the network with an encoder-decoder architecture. The prototype layer stores weights which are close to encoded training samples, and a decoder is used to visualize them. However, their model fails to generate realistic visualizations for natural images. Thus [7] proposed to learn prototypes for each class and visualized them by tracing them back to the input images without a decoder. Our work is inspired by [7], but where their work is limited to 2D images and provides only one-level explanations we extend it to multi-level explanations for videos.

[36] focuses on reducing the number of prototypes for each class by finding shared prototypes among classes. [28] enhances the prototypical explanations by adding textual explanations to explain prototypes. [49] introduced a different similarity metric for computing similarities between prototypes and image patches. They also introduced a loss function to enhance the diversity of prototypes within a class. Deformable ProtoPNet [9] learns spatially flexible prototypes to capture pose and context variations in the input. All previous prototype-based explanation methods provide explanations without considering the hierarchical relations between classes on well-defined image CUB birds [48] and Stanford cars [20] datasets. In contrast inspired by the human way of explanations we consider hierarchical relations between classes while learning prototypes for each class for video datasets.

Most closely related to our work are [29, 45]. [45] introduced a dynamic prototype network (DPNet) for finding temporal artifacts and unnatural movements in deep fake videos. However, the goal of DPNet is different from ours with only two target classes fake/real making the task easier. [29] introduced neural prototype trees by combining CNN architecture with the soft binary trees for providing local and global explanations. However, as the number of prototypes depends upon the size of the tree learning a Pro-

toTree becomes computationally expensive. Our proposed multi-level explanations do not add any extra computational complexity to the training.

2.3. Hyperbolic Embeddings

[30] demonstrated that hyperbolic embeddings can learn hierarchical tree-like structures. Later on, the effectiveness of hyperbolic embeddings have been shown for textual [11, 44, 55] to visual data [1, 12, 18, 26]. Hyperbolic embeddings have also been used for zero-shot learning [10, 25] and for video action recognition [26, 43]. The hierarchical relationship between videos and the hierarchical way of explaining decisions for humans calls for the need of using hyperbolic spaces. In this work, we utilize hyperbolic embeddings for learning hierarchical prototypes to provide human-like explanations for video action recognition.

3. Hierarchical Action Embeddings

Incorporating the prior hierarchical knowledge about actions into the network requires that we represent them as embeddings. In this section we detail how to learn those action embeddings in hyperbolic space, in the next section, we explain how to learn hierarchical prototypes that are optimized by aligning them to the action embeddings in hyperbolic space. Given the set of action classes $\mathcal{A} = \{1, 2, \dots, |\mathcal{A}|\}$, in hierarchical action recognition we also consider their ancestor classes $\mathcal{H} = \{|\mathcal{A}| + 1, |\mathcal{A}| + 2, \dots, |\mathcal{A}| + |\mathcal{H}|\}$, which allows us to construct a hierarchical tree with three levels, i.e., grandparent, parent, and child (see Figure 2 right). This process of embedding the hierarchies is performed once, offline, per dataset. However, this process can easily be repeated for alternative hierarchies.

Learning Action Embeddings. We map the action hierarchy $\mathcal{A} \cup \mathcal{H}$ into the shared hyperbolic space \mathbb{D}^n to obtain hierarchical action embeddings, which are used as action class templates in the next section. Let $\mathcal{P} = \{(u, v) | u = \phi(v)\}$ be the positive pair of v and its parent $\phi(v)$ and $\mathcal{N} = \{(u', v') | u' \neq \phi(v')\}$ be the negative pairs. The discriminative loss akin to [26]:

$$\mathcal{L}(\mathcal{P}, \mathcal{N}, \Phi) = \mathcal{L}_H(\mathcal{P}, \mathcal{N}) + \lambda \cdot \mathcal{L}_S(\Phi), \quad (1)$$

where Φ stands for class templates matrix and its c -th column Φ_c is the template vector of class c in \mathbb{D}^n . For the loss function, \mathcal{L}_H encourages the preservation of parent-child relations and \mathcal{L}_S enforces separation among different sub-hierarchies. The first part \mathcal{L}_H is akin to [31], where the wrongly positioned child-parent pairs will be penalized:

$$\mathcal{L}_H(\mathcal{P}, \mathcal{N}) = \sum_{(\mathbf{u}, \mathbf{v}) \in \mathcal{P}} \log \left(\frac{e^{-d(\mathbf{u}, \mathbf{v})}}{\sum_{(\mathbf{u}', \mathbf{v}') \in \mathcal{N}} e^{-d(\mathbf{u}', \mathbf{v}')}} \right), \quad (2)$$

where $-d(\mathbf{u}, \mathbf{v})$ is the hyperbolic distance between two action embeddings \mathbf{u} and \mathbf{v} , which can be written in short-

hand notation:

$$d(\mathbf{v}, \mathbf{u}) := 2 \operatorname{arctanh}(\|-\mathbf{v} \oplus \mathbf{u}\|), \quad (3)$$

where \oplus indicates the Möbius addition [47] in 1-curved hyperbolic space \mathbb{D}^n .

In the second part, we encourage the separation among sibling relationships, where we update Φ with separation loss:

$$\mathcal{L}_S(\Phi) = - \sum_{i \in |\mathcal{A}|} \|\tilde{\Phi}_i^T \tilde{\Phi}_i\|_F + \gamma \|(\hat{\Phi}_i \hat{\Phi}_i^T - \mathbf{I})\|_F, \quad (4)$$

where $\hat{\Phi}$ consists of the non-sibling vectors with respect to action class i while $\tilde{\Phi}$ consists of i 's sibling vectors.

After learning with the above objectives, we obtain Φ , a matrix of action template vectors including both actions \mathcal{A} and ancestor (parent and grandparent) actions \mathcal{H} .

4. Hierarchical ProtoPNet

Figure 2 gives an overview of our proposed Hierarchical ProtoPNet for video action recognition. Our Hierarchical ProtoPNet consists of a 3D-CNN backbone f for extracting features from the video frames, and a prototype layer g_p for learning prototypes for each frame. The prototype layer is followed by a fully connected layer h that combines the prototype similarity scores maps them to the shared hyperbolic space through exponential mapping. Prior knowledge about the relations between actions, in the form of the action hierarchy, are projected to the shared space through discriminative embeddings, as described in Section 3. Subsequently, we use hyperbolic learning to obtain hierarchical prototypes that enable multi-level explainability.

4.1. Feature Extraction

As the backbone architecture, we use the video action classification network 3D-Resnet [14]. For each input video $v \in \mathbb{R}^{W \times H \times T \times 3}$ with T frames it extracts video features $Z \in \mathbb{R}^{W_0 \times H_0 \times T_0 \times D}$ with the spatial resolution $W_0 \times H_0$, frames T_0 and channels D . A key aspect of this backbone is that $T_0 < T$ due to temporal pooling, as such the features Z are extracted for segments rather than individual frames. Because of the temporal pooling, the prototypes learned by our Hierarchical ProtoPNet are spatiotemporal thereby explaining which parts of the segment are indicative of the action in the video.

4.2. Prototype Layer

Given the features extracted from the 3D-Resnet Z , two layers of $1 \times 1 \times 1$ convolutions with the LeakyReLU activations are added for adjusting the number of channels for the top layer. For each child \mathcal{A} and its parent \mathcal{H} action, the network learns m and n prototypes respectively $P = \{p_j\}_{j=1}^{m+n}$, whose shape is $W_1 \times H_1 \times T_1 \times D$ with

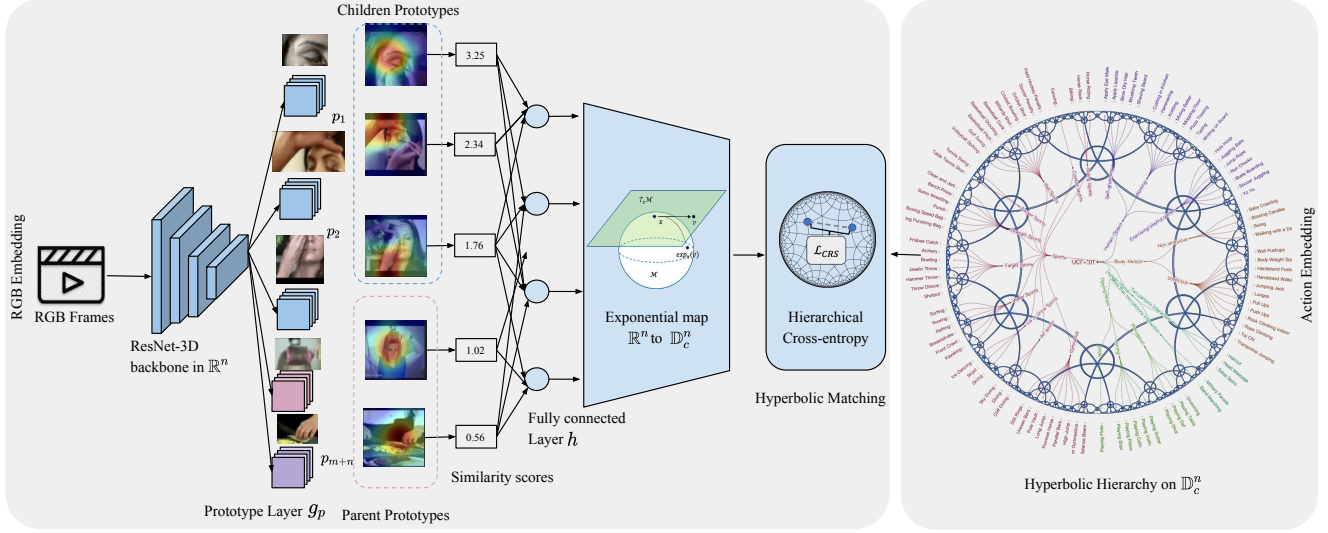


Figure 2. **Overview of the Hierarchical ProtoPNet.** The Resnet-3D backbone extracts video features and the prototype layer learns prototypes for children and parents, these prototypes are then converted to a single similarity score through max pooling. Finally, scores are converted from \mathbb{R}^n to \mathbb{D}^n through a fully connected layer followed by an exponential map, to the shared hyperbolic space for Hierarchical learning. Actions are mapped onto the shared hyperbolic space by learning a discriminative embedding on \mathbb{D}^n .

$W_1 \leq W_0$, $H_1 \leq H_0$ and $T_1 \leq T_0$. As such each prototype represents a spatiotemporal part of the video. Given the convolutional output $Z = f(v)$ and prototypes p a prototype layer g_p computes the distances between each prototype p_j and the patches from Z and converts them to the similarity scores using

$$g_p(p_j, Z) = \max_{z \in Z} \log \frac{(\|z - p_j\|_2^2 + 1)}{(\|z - p_j\|_2^2 + \epsilon)}, \epsilon > 0 \quad (5)$$

The distances between each prototype and the patch determine the extent to which a prototype is present in the input. In contrast with the prior ProtoPNet architectures, we multiply similarity scores with the weights of a fully connected layer h to obtain embeddings to be projected in the hyperbolic joint space for learning hierarchical prototypes.

4.3. Hierarchical Video Embeddings.

The embeddings $\mathbf{h} = h(g_p(p, f(v)))$ obtained from the prototype layer are in the Euclidean space and can not be directly mapped into the hyperbolic embedding space, therefore, we use exponential mapping [11] to map video embeddings into the hyperbolic space.

$$\exp_{\mathbf{x}}(\mathbf{h}) = \mathbf{x} \oplus \left(\tanh\left(\frac{\|\mathbf{h}\|}{1 - \|\mathbf{x}\|^2}\right) \frac{\mathbf{h}}{\|\mathbf{h}\|} \right) \quad (6)$$

where \oplus indicates the 1-curved Mobius addition, \mathbf{x} is the tangent point connecting tangent space $\mathcal{T}_0 \mathbb{D}^n$ to \mathbb{D}^n . Different values of x lead to different tangent spaces, to avoid any ambiguities we set $\mathbf{x} = \mathbf{0}$ and project the video embeddings

to the hyperbolic space for matching with the hierarchical actions.

4.4. Training Hierarchical ProtoPNet

Our training process consists of a multi-step procedure: initially epochs we perform warm-up of the newly added layers. Following the warm-up, we train the entire network end-to-end. Every 10 epochs we perform prototype projection, i.e., updating the prototype layer only, followed by a phase of fine-tuning the layers after the prototype layer.

Video and Action Matching in the Hyperbolic Space

We aim to learn a latent space where patches important for classification are clustered around similar prototypes. In order to learn hierarchical prototypes we optimize the prototypes $P = \{p_j\}_{j=1}^{m+n}$ to match videos to hyperbolic action embeddings, hence our optimization is supervised by $\Phi \in \mathbb{D}^{n \times (|\mathcal{A}|)}$. Let $\{(v_i, y_i)\}_{i=1}^N$ be the training set, where $v \in \mathbb{R}^{W \times H \times T \times 3}$ and $y_i \in \mathcal{A}$. Our goal is to solve:

$$\mathcal{L}_{crs} + \lambda_1 \mathcal{L}_{cls} + \lambda_2 \mathcal{L}_{sep} \quad (7)$$

Hierarchical Cross Entropy. The first term in our loss is the hierarchical cross-entropy loss \mathcal{L}_{crs} which penalizes the misclassification defined as:

$$\mathcal{L}_{crs} = \frac{1}{N} \sum_{i=1}^N \sum_{k=1}^K y_{ik} \log p(y = k|v) \quad (8)$$

The softmax in the cross entropy is defined as the negative distance between video embeddings and the hierarchical ac-

tion embeddings in the hyperbolic space:

$$p(y = k|v) = \frac{\exp(-d(\mathbf{h}_e), \Phi_k)}{\sum_{k'} \exp(-d(\mathbf{h}_e), \Phi_{k'}))}, \quad (9)$$

where $\mathbf{h}_e = \exp_0(\mathbf{h})$ is applying exponential map to the prototype output \mathbf{h} .

Hierarchical Clustering. Our hierarchical clustering cost encourages input images to have at least one patch from features to be closer to a child, parent or grandparent class prototype.

$$\mathcal{L}_{cls} = \frac{1}{N} \sum_{i=1}^N \min_{j: p_j \in P_{|\mathcal{A}|+|\mathcal{H}|}} \min_{z \in \text{patches}(f(v_i))} \|z - p_j\|_2^2 \quad (10)$$

Hierarchical Separation. Our hierarchical separation cost encourages the latent patches of the images to stay away from the prototypes not belonging to the same child class or parent class or grandparent class.

$$\mathcal{L}_{sep} = -\frac{1}{N} \sum_{i=1}^N \min_{j: p_j \notin P_{|\mathcal{A}|+|\mathcal{H}|}} \min_{z \in \text{patches}(f(v_i))} \|z - p_j\|_2^2 \quad (11)$$

4.5. Prototype Projection

We project prototypes onto the closest video features from the training videos. We do so for child, parent, and grandparent action categories. Mathematically, for a prototype p_j from child, parent or grandparent class i.e. $p_j \in P_{|\mathcal{A}|+|\mathcal{H}|}$, we update the prototype layer as:

$$p_j \leftarrow \underset{z \in \mathcal{Z}_j}{\operatorname{argmin}} \|z - p_j\|_2 \quad (12)$$

where $\mathcal{Z}_j = \{\tilde{z} : \tilde{z} \in \text{patches}(f(v_i)) \forall i \text{ s.t. } y_i = |\mathcal{A}| + |\mathcal{H}|\}$. Our prototype layer is updated not only with the prototypes belonging to the child class but also with the parent and grandparent classes enabling the learning of hierarchical relations between classes.

4.6. Prototype Visualization

To construct the visualizations the learned prototypes are mapped to the spatio-temporal input space. We select the patch which highly activates for the prototype p_j by forwarding the input v through the network and upsampling the activation map generated by the prototype layer $g_p(p_j, Z)$ both spatially and temporally (for videos). We visualize p_j for child, parent, and grandparent classes providing explanations at all levels of the hierarchy.

5. Experimental Setup

5.1. Datasets

To evaluate our Hierarchical ProtoPNet for videos we conduct experiments on two video datasets: UCF-101 [40]

and Activity-Net1.3 [5]. For UCF-101 only one level action hierarchy is available with the dataset, therefore we define additional levels to complement the hierarchy. For ActivityNet we used the hierarchy protocol provided with the dataset. All the hierarchies are made available together with our implementation.

Hierarchical UCF-101. UCF-101 [40] contains 13,320 videos belonging to 101 action categories with a total length of 27 hours. We define two additional levels of hierarchy with the number of classes at level one, two, and three being 5, 20, and 101 respectively. The classes at the third level of the hierarchy are the 101 original classes of the dataset. The full hierarchy is included in the supplementary material.

Hierarchical ActivityNet. ActivityNet [5] contains 14,950 untrimmed videos with each video consisting of one or more action segments belonging to 200 action classes with a total length of approximately 648 hours. We use 10,024 videos for training and 4,926 for validation. We follow [14] and train and test our model on trimmed videos to determine video-level accuracy. We follow [26] to define the class-level action hierarchies using the hierarchies that come with the dataset. It contains 200, 38, and 6 classes in level one, two, and three respectively.

5.2. Implementation Details

The hierarchical action embeddings are generated by training the model with Reimannian Adam optimizer [3], implemented with *geoopt* and Pytorch [33]. Apart from the one-time offline step of generating the hierarchical action embedding our Hierarchical ProtoPNet is trained in an end-to-end fashion. For feature extraction, we used Resnet-3D-18 [14] pre-trained on Kinetics [6] and added two 1×1 convolutional layers with the LeakyReLU, a prototype layer and the final embedding layer. We perform prototype projection and visualization every 10 epochs.

We report results on two variations of our Hierarchical ProtoPNet: Hierarchical ProtoPNet with the hyperbolic cross-entropy loss and Hierarchical ProtoPNet CPG (child, parent and grandparent) with hyperbolic cross-entropy loss. For the CPG variant, we compare between prototype projection with 5 prototypes per class and 10 prototypes per class, to explore whether this additional supervision makes it possible to use fewer prototypes. For comparison, we adapt ProtoPNet [7] to videos by replacing the 2D ResNet backbone with a 3D ResNet backbone.

Evaluation Metrics. We report the performance at both clip level and video level. The clip level accuracy is the rate of correct prediction of each clip, while the video level accuracy is the majority vote of the predictions over all the clips within the video. Additionally, to show the benefit of using hierarchical learning, we report accuracy for three metrics: the class accuracy is calculated as the rate

	Network	Accuracy	Sibling Accuracy	Cousin Accuracy	# of prototypes per class
Non-Interpretable Models	3D-Resnet [14]	83.34	89.73	93.62	-
	Resnet-Hyperbolic [26]	82.64	89.99	93.28	-
Interpretable Models	ProtoPNet [7]	78.30	85.92	90.98	10
	Hierarchical ProtoPNet	79.49	88.60	92.79	10
	Hierarchical ProtoPNet CPG	79.45	88.88	92.73	5
	Hierarchical ProtoPNet CPG	80.40	89.30	93.02	10

Table 1. **Clip level accuracy comparison for different models on UCF-101 videos.** We observe that our hierarchical ProtoPNet CPG with 10 prototypes per class recovers the drop due to accuracy-explainability trade-off significantly while providing multi-level explanations.

of correct prediction in the hierarchical space 0-hop away from the ground-truth, the sibling accuracy as the rate of correct prediction 2-hops away from the ground-truth, and the cousin accuracy as the 4-hops correct prediction rate. Higher performance on the sibling and cousin metrics indicates that misclassifications are to hierarchically nearby, and therefore, semantically similar classes.

6. Experiments

6.1. Recognition Accuracy

Non-Interpretable Models. The performance of non-interpretable models on UCF-101 and ActivityNet are shown in the top two rows of Tables 1, 2, and 3. For fair comparison both non-interpretable models, a regular Resnet [14] and a hyperbolic Resnet [26], are trained end-to-end with the same data augmentations and an equal number of epochs. The only difference between the two non-interpretable models is that for the Resnet model the categories are separated through euclidean hyperplanes while the Resnet-Hyperbolic utilizes hyperbolic embedding space to separate categories. Our results for UCF-101 show that both a regular Resnet and the hyperbolic Resnet perform similarly at clip level (Table 1) and video level (Table 3).

For ActivityNet the clip-level class accuracy (Table 2) is comparable across both networks, however, due to the hierarchical learning of hyperbolic Resnet it shows better sibling and cousin accuracy, additionally, it shows an improvement for class accuracy at the video level (see Table 3). Overall, we see comparable performance for the non-interpretable networks on UCF-101 and improvements for the Hyperbolic networks on ActivityNet.

Interpretable Models. The performance of interpretable models on UCF-101 and ActivityNet are shown in the bottom four rows of Table 1, 2, and 3. We report the results for a regular ProtoPNet [7] adapted for videos and the variations of our Hierarchical ProtoPNet.

For UCF-101, with a regular ProtoPNet with 10 prototypes per class, the accuracy drops considerably: the clip-level class accuracy drops to 78.30 and the video-level accu-

racy to 84.48. This is because of the explainability-accuracy trade-off common in explainable-AI, also reported in [7]. In contrast, our hierarchical ProtoPNet is much less affected and recovers the drop by 1.19 for class accuracy, 2.68, and 1.81 for sibling and cousin accuracies respectively. Our Hierarchical-ProtoPNet CPG with 5 prototypes per class also shows similar improvement in performance, however, increasing the number of prototypes to 10 per class improves the performance by 2.10, 3.38, and 2.04 for class, sibling, and cousin accuracies respectively. Moreover, the performance at the video level reaches 86.22 (see Table 3). Hence, all three variations of our proposed hierarchical ProtoPNet reduce the accuracy drop.

On ActivityNet (see Table 2) we observe a clear accuracy-explainability trade-off for the regular ProtoPNet, with drops in both the clip and video level accuracies. However, whilst our Hierarchical ProtoPNet shows a similar drop in class accuracy we can observe that it partially recovers from this drop on the sibling and cousin metrics. This behavior holds for both the Hierarchical ProtoPNet CPG with 5 prototypes, and for CPG variant with 10 prototypes per class we even see improvements for the sibling and cousin metrics of 1.19 and 1.3 respectively. Whilst ActivityNet remains challenging, an improvement in sibling and cousin accuracies is directly beneficial to the explainability as demonstrated in Section 6.2.

Hence, we can observe that on both datasets our Hierarchical ProtoPNet is less affected by the accuracy-explainability trade-off whilst also providing multi-level explanations.

6.2. Visual Explanations

Multi-level Explanations. Figure 3 shows an example of multi-level explanations provided by our Hierarchical ProtoPNet. Our model learns to represent the video clip features as hierarchical prototypes that belong to grandparent, parent and child classes. For example, in Figure 3 our model has learned prototypes (only one out of ten prototypes shown for better presentation) from the grandparent class *playing instruments*, parent class *percussion* and the

	Network	Accuracy	Sibling Accuracy	Cousin Accuracy	# of prototypes per class
Non-Interpretable Models	3D-Resnet [14]	49.99	51.59	63.88	-
	Hyperbolic-Resnet [26]	49.95	52.03	65.44	-
Interpretable Models	ProtoPNet [7]	46.06	47.74	61.67	10
	Hierarchical ProtoPNet	46.02	48.76	62.77	10
	Hierarchical ProtoPNet CPG	45.67	48.72	62.84	5
	Hierarchical ProtoPNet CPG	46.26	48.93	62.97	10

Table 2. **Clip level accuracy comparison for different models on ActivityNet videos.** We observe that our hierarchical ProtoPNet CPG with 10 prototypes per class recovers the drop for siblings and cousins and shows comparable performance with regular ProtoPNet for class accuracy while providing multi-level explanations.

	Network	UCF-101 Accuracy	ActivityNet Accuracy	# of prototypes per class
Non-Interpretable Models	3D-Resnet [14]	87.92	69.15	-
	Resnet-Hyperbolic [26]	87.15	70.19	-
Interpretable Models	ProtoPNet [7]	84.48	66.46	10
	Hierarchical ProtoPNet	84.03	64.66	10
	Hierarchical ProtoPNet CPG	84.87	63.82	5
	Hierarchical ProtoPNet CPG	86.22	66.48	10

Table 3. **Video level accuracy comparison for different models on UCF-101 and ActivityNet videos.** We observe that our hierarchical ProtoPNet CPG with 10 prototypes per class recovers the drop at video level significantly for UCF-101 and shows comparable performance with the regular ProtoPNet for ActivityNet while providing multi-level explanations.

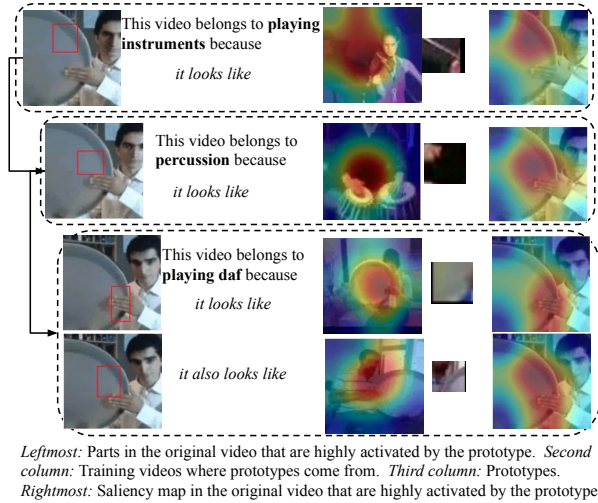


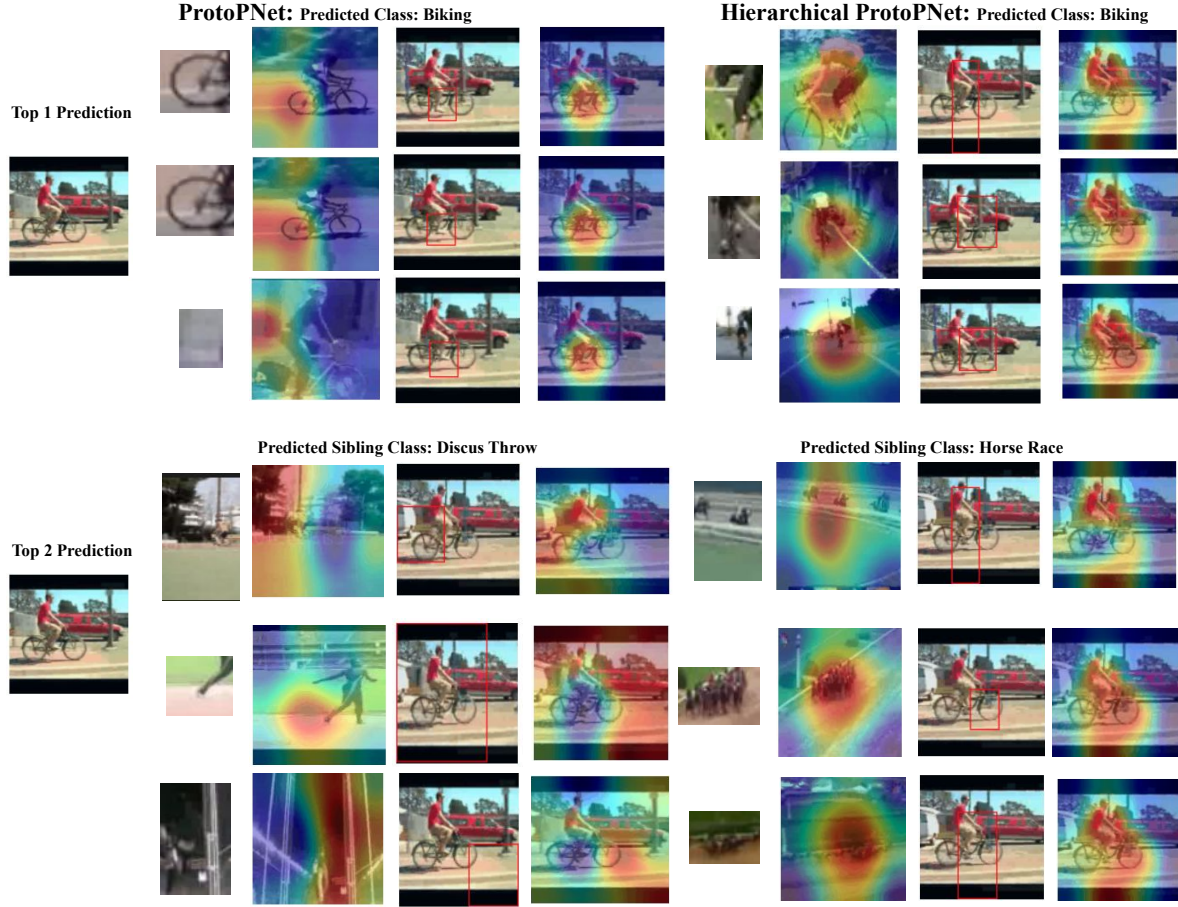
Figure 3. **Multi-level Explanations.** Schematic representation of the hierarchical prototype-based reasoning process of our proposed Hierarchical ProtoPNet.

action class *playing daf*. We see the similarity between the grandparent and original video in the posture of players and hand movement, for the parent we observe the similarity in the hands movement, and finally the prototypes for the play-

ing daf class show greater similarity for both the instrument and the hand movements.

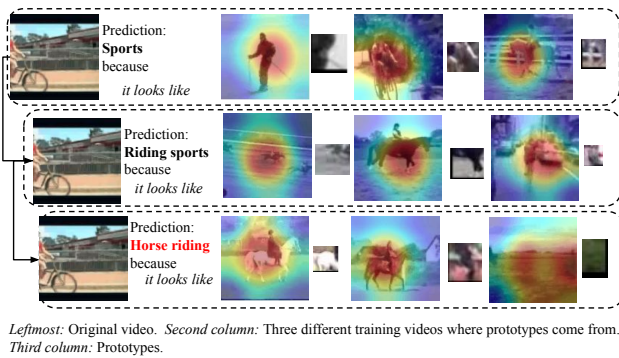
Effectiveness of Multi-level Explanations. The learned prototypes of the regular ProtoPNet with our Hierarchical ProtoPNet are contrasted in Figure 4. In Figure 4 top, we observe that the top prediction by both the networks regular ProtoPNet and Hierarchical-ProtoPNet CPG are correct (i.e., *biking*), however the learned prototypes for ProtoPNet focus only on the tyres or the background. While for our Hierarchical ProtoPNet the prototypes are diverse, focusing on the tyre and pedals. Moreover, the top 2 prediction in the bottom half of Figure 4 for the ProtoPNet is *Discus Throw* which is non-related to biking according to human intuition, while for the hierarchical ProtoPNet it is *Horse Racing* which relates to biking as it is a riding sport. We observe that the prototypes for *Discus throw* are random and when we visualize the area highly activated by those prototypes, it either focuses on the background or ground (see Figure 4 last two rows). Instead for our Hierarchical ProtoPNet, the top 2 prediction is *Horse Racing* and the prototypes predominantly focus on the riders.

In Figure 5 we show another scenario where the multi-level explanations are useful. We see that the original video is misclassified into *horse riding* class, however, for the more abstract explanations we can observe that its par-



Leftmost: Original Video Frame. Second column: Prototypes. Third column: Training videos where prototypes come from. Fourth column: Parts in the original video that are highly activated by the prototype. Rightmost: Saliency map in the original video that are highly activated by the prototype. (*Repeat for hierarchical ProtoPNet).

Figure 4. **Effectiveness in contrast to regular ProtoPNet.** The comparison between regular ProtoPNet and our Hierarchical ProtoPNet shows that our model learns more diverse prototypes in a hierarchical way and the prototypes for the siblings are also intuitive for humans.



Leftmost: Original video. Second column: Three different training videos where prototypes come from. Third column: Prototypes.

Figure 5. **Effectiveness in case of failure.** Our multi-level explanations provide useful information even in the case of misclassification through the prototypes learned for parent and grandparent classes.

ent class *riding sports* and grandparent class *sports* are cor-

rectly recognized. Hence our hierarchical explanations give us useful information even in the case of misclassification.

7. Conclusion

In this work, we proposed Hierarchical ProtoPNet for video action recognition. By learning hierarchical prototypes we are able to provide explanations at multiple levels of granularity, not only explaining why it is classified as a certain class, but also what spatiotemporal parts contribute to it belonging to parent categories. Our results show that Hierarchical ProtoPNet outperforms a prior non-hierarchical approach on UCF-101, whilst performing equally well on ActivityNet. Additionally, we demonstrate our multi-level explanations that make it possible to see which spatiotemporal parts contribute to grandparent, parent, and class-level classifications. Our hierarchical approach thereby provides richer explanations whilst compromising less performance to gain explainability.

References

- [1] Mina Ghadimi Atigh, Julian Schoep, Erman Acar, Nanne van Noord, and Pascal Mettes. Hyperbolic image segmentation. In *Proceedings of the IEEE/CVF Conference on Computer Vision and Pattern Recognition*, pages 4453–4462, 2022. [2](#), [3](#)
- [2] Sarah Adel Bargal, Andrea Zunino, Donghyun Kim, Jianming Zhang, Vittorio Murino, and Stan Sclaroff. Excitation backprop for rnns. In *Proceedings of the IEEE Conference on Computer Vision and Pattern Recognition*, pages 1440–1449, 2018. [2](#)
- [3] Gary Bécigneul and Octavian-Eugen Ganea. Riemannian adaptive optimization methods. *arXiv preprint arXiv:1810.00760*, 2018. [5](#)
- [4] Luca Bertinetto, Jack Valmadre, Joao F Henriques, Andrea Vedaldi, and Philip HS Torr. Fully-convolutional siamese networks for object tracking. In *European conference on computer vision*, pages 850–865. Springer, 2016. [1](#), [2](#)
- [5] Fabian Caba Heilbron, Victor Escorcia, Bernard Ghanem, and Juan Carlos Niebles. Activitynet: A large-scale video benchmark for human activity understanding. In *Proceedings of the IEEE conference on computer vision and pattern recognition*, pages 961–970, 2015. [5](#), [11](#)
- [6] Joao Carreira and Andrew Zisserman. Quo vadis, action recognition? a new model and the kinetics dataset. In *proceedings of the IEEE Conference on Computer Vision and Pattern Recognition*, pages 6299–6308, 2017. [1](#), [2](#), [5](#)
- [7] Chaofan Chen, Oscar Li, Daniel Tao, Alina Barnett, Cynthia Rudin, and Jonathan K Su. This looks like that: deep learning for interpretable image recognition. *Advances in neural information processing systems*, 32, 2019. [1](#), [2](#), [5](#), [6](#), [7](#)
- [8] Bhuwan Dhingra, Christopher J Shallue, Mohammad Norouzi, Andrew M Dai, and George E Dahl. Embedding text in hyperbolic spaces. *arXiv preprint arXiv:1806.04313*, 2018. [2](#)
- [9] Jon Donnelly, Alina Jade Barnett, and Chaofan Chen. Deformable protopnet: An interpretable image classifier using deformable prototypes. In *Proceedings of the IEEE/CVF Conference on Computer Vision and Pattern Recognition*, pages 10265–10275, 2022. [1](#), [2](#)
- [10] Pengfei Fang, Mehrtash Harandi, and Lars Petersson. Kernel methods in hyperbolic spaces. In *Proceedings of the IEEE/CVF International Conference on Computer Vision*, pages 10665–10674, 2021. [3](#)
- [11] Octavian Ganea, Gary Bécigneul, and Thomas Hofmann. Hyperbolic entailment cones for learning hierarchical embeddings. In *International Conference on Machine Learning*, pages 1646–1655. PMLR, 2018. [3](#), [4](#)
- [12] Mina Ghadimi Atigh, Martin Keller-Ressel, and Pascal Mettes. Hyperbolic busemann learning with ideal prototypes. *Advances in Neural Information Processing Systems*, 34:103–115, 2021. [2](#), [3](#)
- [13] Sadaf Gulshad and Arnold Smeulders. Explaining with counter visual attributes and examples. In *Proceedings of the 2020 International Conference on Multimedia Retrieval, ICMR '20*, 2020. [1](#), [2](#)
- [14] Kensho Hara, Hirokatsu Kataoka, and Yutaka Satoh. Can spatiotemporal 3d cnns retrace the history of 2d cnns and imagenet? In *Proceedings of the IEEE Conference on Computer Vision and Pattern Recognition (CVPR)*, pages 6546–6555, 2018. [1](#), [2](#), [3](#), [5](#), [6](#), [7](#)
- [15] Lisa Anne Hendricks, Ronghang Hu, Trevor Darrell, and Zeynep Akata. Grounding visual explanations. In *ECCV*, September 2018. [1](#), [2](#)
- [16] Andrej Karpathy, Justin Johnson, and Li Fei-Fei. Visualizing and understanding recurrent networks. *arXiv preprint arXiv:1506.02078*, 2015. [2](#)
- [17] Andrej Karpathy, George Toderici, Sanketh Shetty, Thomas Leung, Rahul Sukthankar, and Li Fei-Fei. Large-scale video classification with convolutional neural networks. In *CVPR*, 2014. [1](#), [2](#)
- [18] Valentin Khrulkov, Leyla Mirvakhabova, Evgeniya Ustinova, Ivan Oseledets, and Victor Lempitsky. Hyperbolic image embeddings. In *Proceedings of the IEEE/CVF Conference on Computer Vision and Pattern Recognition*, pages 6418–6428, 2020. [3](#)
- [19] Jinkyu Kim, Anna Rohrbach, Trevor Darrell, John Canny, and Zeynep Akata. Textual explanations for self-driving vehicles. In *ECCV*, September 2018. [1](#), [2](#)
- [20] Jonathan Krause, Michael Stark, Jia Deng, and Li Fei-Fei. 3d object representations for fine-grained categorization. In *4th International IEEE Workshop on 3D Representation and Recognition (3dRR-13)*, Sydney, Australia, 2013. [2](#)
- [21] Oscar Li, Hao Liu, Chaofan Chen, and Cynthia Rudin. Deep learning for case-based reasoning through prototypes: A neural network that explains its predictions. In *Proceedings of the AAAI Conference on Artificial Intelligence*, volume 32, 2018. [1](#), [2](#)
- [22] Yanan Li and Donghui Wang. Zero-shot learning with generative latent prototype model. *arXiv preprint arXiv:1705.09474*, 2017. [2](#)
- [23] Zhenqiang Li, Weimin Wang, Zuoyue Li, Yifei Huang, and Yoichi Sato. Towards visually explaining video understanding networks with perturbation. In *Proceedings of the IEEE/CVF Winter Conference on Applications of Computer Vision*, pages 1120–1129, 2021. [1](#), [2](#)
- [24] Xinmiao Lin, Wentao Bao, Matthew Wright, and Yu Kong. Gradient frequency modulation for visually explaining video understanding models. *arXiv preprint arXiv:2111.01215*, 2021. [2](#)
- [25] Shaoteng Liu, Jingjing Chen, Liangming Pan, Chong-Wah Ngo, Tat-Seng Chua, and Yu-Gang Jiang. Hyperbolic visual embedding learning for zero-shot recognition. In *Proceedings of the IEEE/CVF conference on computer vision and pattern recognition*, pages 9273–9281, 2020. [3](#)
- [26] Teng Long, Pascal Mettes, Heng Tao Shen, and Cees GM Snoek. Searching for actions on the hyperbole. In *Proceedings of the IEEE/CVF Conference on Computer Vision and Pattern Recognition*, pages 1141–1150, 2020. [2](#), [3](#), [5](#), [6](#), [7](#)
- [27] Scott M Lundberg and Su-In Lee. A unified approach to interpreting model predictions. *Advances in neural information processing systems*, 30, 2017. [2](#)
- [28] Meike Nauta, Annemarie Jutte, Jesper Provoost, and Christin Seifert. This looks like that, because... explaining prototypes

- for interpretable image recognition. In *Joint European Conference on Machine Learning and Knowledge Discovery in Databases*, pages 441–456. Springer, 2021. 2
- [29] Meike Nauta, Ron van Bree, and Christin Seifert. Neural prototype trees for interpretable fine-grained image recognition. In *Proceedings of the IEEE/CVF Conference on Computer Vision and Pattern Recognition*, pages 14933–14943, 2021. 2
- [30] Maximillian Nickel and Douwe Kiela. Poincaré embeddings for learning hierarchical representations. *Advances in neural information processing systems*, 30, 2017. 3
- [31] Maximilian Nickel and Douwe Kiela. Poincaré Embeddings for Learning Hierarchical Representations. In *NeurIPS*, 2017. 3
- [32] Frederik Pahde, Mihai Puscas, Tassilo Klein, and Moin Nabi. Multimodal prototypical networks for few-shot learning. In *Proceedings of the IEEE/CVF Winter Conference on Applications of Computer Vision*, pages 2644–2653, 2021. 2
- [33] Adam Paszke, Sam Gross, Francisco Massa, Adam Lerer, James Bradbury, Gregory Chanan, Trevor Killeen, Zeming Lin, Natalia Gimelshein, Luca Antiga, et al. Pytorch: An imperative style, high-performance deep learning library. *Advances in neural information processing systems*, 32, 2019. 5
- [34] Xiaojiang Peng and Cordelia Schmid. Multi-region two-stream r-cnn for action detection. In *European conference on computer vision*, pages 744–759. Springer, 2016. 1, 2
- [35] Marco Tulio Ribeiro, Sameer Singh, and Carlos Guestrin. ”why should i trust you?” explaining the predictions of any classifier. In *Proceedings of the 22nd ACM SIGKDD international conference on knowledge discovery and data mining*, pages 1135–1144, 2016. 2
- [36] Dawid Rymarczyk, Łukasz Struski, Jacek Tabor, and Bartosz Zieliński. Protopshare: Prototype sharing for interpretable image classification and similarity discovery. *arXiv preprint arXiv:2011.14340*, 2020. 2
- [37] Karen Simonyan and Andrew Zisserman. Two-stream convolutional networks for action recognition in videos. *Advances in neural information processing systems*, 27, 2014. 1, 2
- [38] Gurkirt Singh, Suman Saha, Michael Sapienza, Philip HS Torr, and Fabio Cuzzolin. Online real-time multiple spatiotemporal action localisation and prediction. In *Proceedings of the IEEE International Conference on Computer Vision*, pages 3637–3646, 2017. 1, 2
- [39] Jake Snell, Kevin Swersky, and Richard Zemel. Prototypical networks for few-shot learning. *Advances in neural information processing systems*, 30, 2017. 2
- [40] Khurram Soomro, Amir Roshan Zamir, and Mubarak Shah. Ucf101: A dataset of 101 human actions classes from videos in the wild. *arXiv preprint arXiv:1212.0402*, 2012. 5, 11
- [41] Alexandros Stergiou, Georgios Kipidis, Grigorios Kalliatakis, Christos Chrysoulas, Ronald Poppe, and Remco Veltkamp. Class feature pyramids for video explanation. In *2019 IEEE/CVF International Conference on Computer Vision Workshop (ICCVW)*, pages 4255–4264. IEEE, 2019. 2
- [42] Alexandros Stergiou, Georgios Kipidis, Grigorios Kalliatakis, Christos Chrysoulas, Remco Veltkamp, and Ronald Poppe. Saliency tubes: Visual explanations for spatio-temporal convolutions. In *2019 IEEE International Conference on Image Processing (ICIP)*, pages 1830–1834. IEEE, 2019. 2
- [43] Dídac Surís, Ruoshi Liu, and Carl Vondrick. Learning the predictability of the future. In *Proceedings of the IEEE/CVF Conference on Computer Vision and Pattern Recognition*, pages 12607–12617, 2021. 3
- [44] Alexandru Tifrea, Gary Bécigneul, and Octavian-Eugen Ganeva. Poincaré glove: Hyperbolic word embeddings. *arXiv preprint arXiv:1810.06546*, 2018. 2, 3
- [45] Loc Trinh, Michael Tsang, Sirisha Rambhatla, and Yan Liu. Interpretable and trustworthy deepfake detection via dynamic prototypes. In *Proceedings of the IEEE/CVF winter conference on applications of computer vision*, pages 1973–1983, 2021. 1, 2
- [46] Tomoki Uchiyama, Naoya Sogi, Koichiro Niinuma, and Kazuhiro Fukui. Visually explaining 3d-cnn predictions for video classification with an adaptive occlusion sensitivity analysis. *arXiv preprint arXiv:2207.12859*, 2022. 2
- [47] Abraham A Ungar. The hyperbolic square and mobius transformations. *Banach Journal of Mathematical Analysis*, 2007. 3
- [48] Catherine Wah, Steve Branson, Peter Welinder, Pietro Perona, and Serge Belongie. The caltech-ucsd birds-200-2011 dataset. 2011. 2
- [49] Jiaqi Wang, Huafeng Liu, Xinyue Wang, and Liping Jing. Interpretable image recognition by constructing transparent embedding space. In *Proceedings of the IEEE/CVF International Conference on Computer Vision*, pages 895–904, 2021. 2
- [50] Limin Wang, Yuanjun Xiong, Zhe Wang, Yu Qiao, Dahua Lin, Xiaoou Tang, and Luc Van Gool. Temporal segment networks: Towards good practices for deep action recognition. In *European conference on computer vision*, pages 20–36. Springer, 2016. 1, 2
- [51] Wenjia Xu, Yongqin Xian, Jiuniu Wang, Bernt Schiele, and Zeynep Akata. Attribute prototype network for zero-shot learning. *Advances in Neural Information Processing Systems*, 33:21969–21980, 2020. 2
- [52] Wenjia Xu, Yongqin Xian, Jiuniu Wang, Bernt Schiele, and Zeynep Akata. Attribute prototype network for any-shot learning. *International Journal of Computer Vision*, pages 1–19, 2022. 2
- [53] Yunlong Yu, Zhong Ji, Jungong Han, and Zhongfei Zhang. Episode-based prototype generating network for zero-shot learning. In *Proceedings of the IEEE/CVF Conference on Computer Vision and Pattern Recognition*, pages 14035–14044, 2020. 2
- [54] Bolei Zhou, Aditya Khosla, Agata Lapedriza, Aude Oliva, and Antonio Torralba. Learning deep features for discriminative localization. In *Proceedings of the IEEE conference on computer vision and pattern recognition*, pages 2921–2929, 2016. 2
- [55] Yudong Zhu, Di Zhou, Jinghui Xiao, Xin Jiang, Xiao Chen, and Qun Liu. Hypertext: Endowing fasttext with hyperbolic geometry. *arXiv preprint arXiv:2010.16143*, 2020. 3

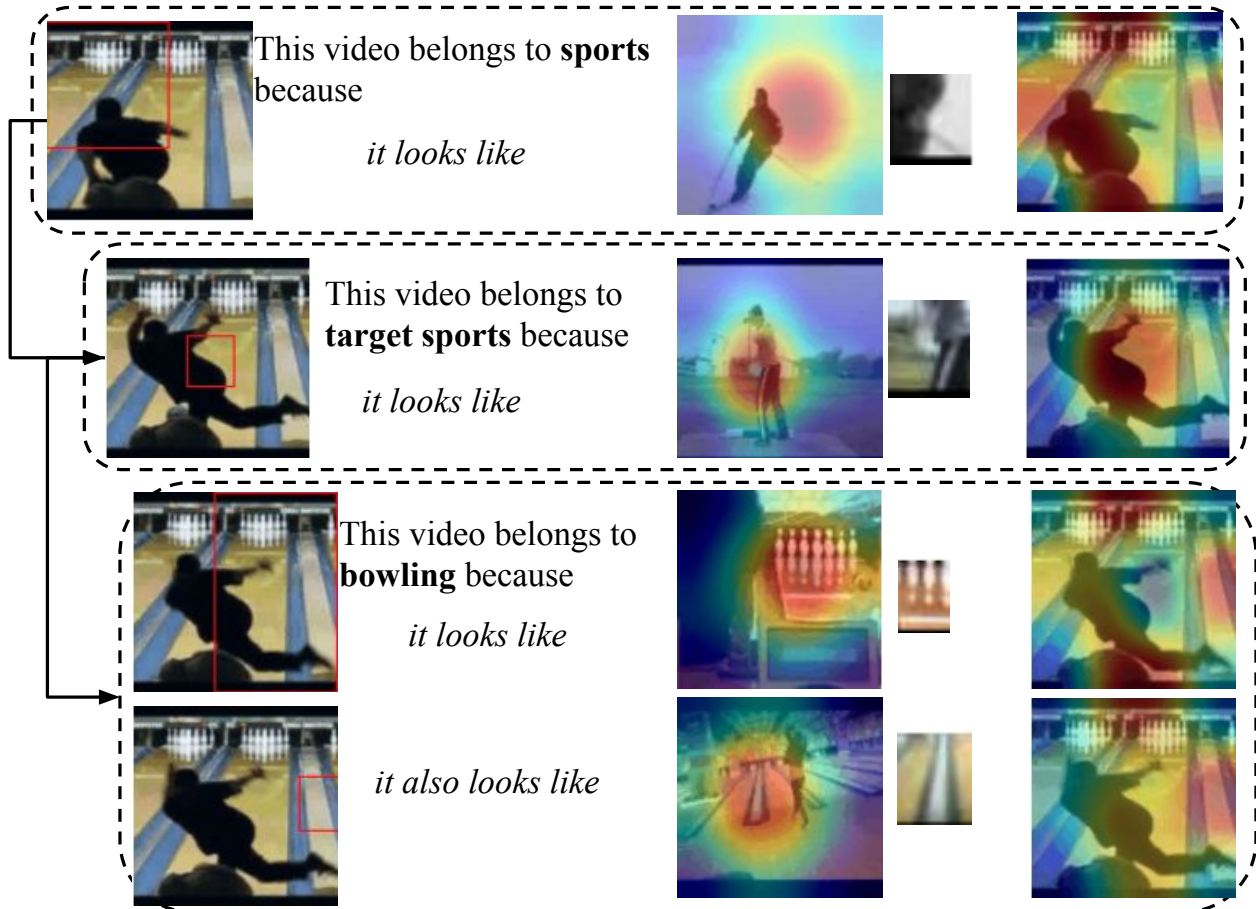
8. Hierarchies for UCF-101 and ActivityNet

Figure 6 and 7 show the hierarchies for UCF-101 [40] and ActivityNet [5] respectively. We define three levels of hierarchy with the number of classes at level one, two, and three being 5, 20, and 101 respectively for UCF-101. For example, one of the grand parent class is *playing music*, parents are *wind*, *string*, *percussion* and children are *playing flute*, *playing guitar*, *drumming* and more. The classes at the third level (i.e., child level) of the hierarchy are the 101 original classes of the dataset.

ActivityNet contains 200, 38, and 6 classes in level one, two, and three respectively (see Figure 7). For instance, one of the grand parent is *personal care* and the parents are *dress up*, *grooming*, *wash up* and children are *putting on shoes*, *getting a haircut*, *shaving* etc.

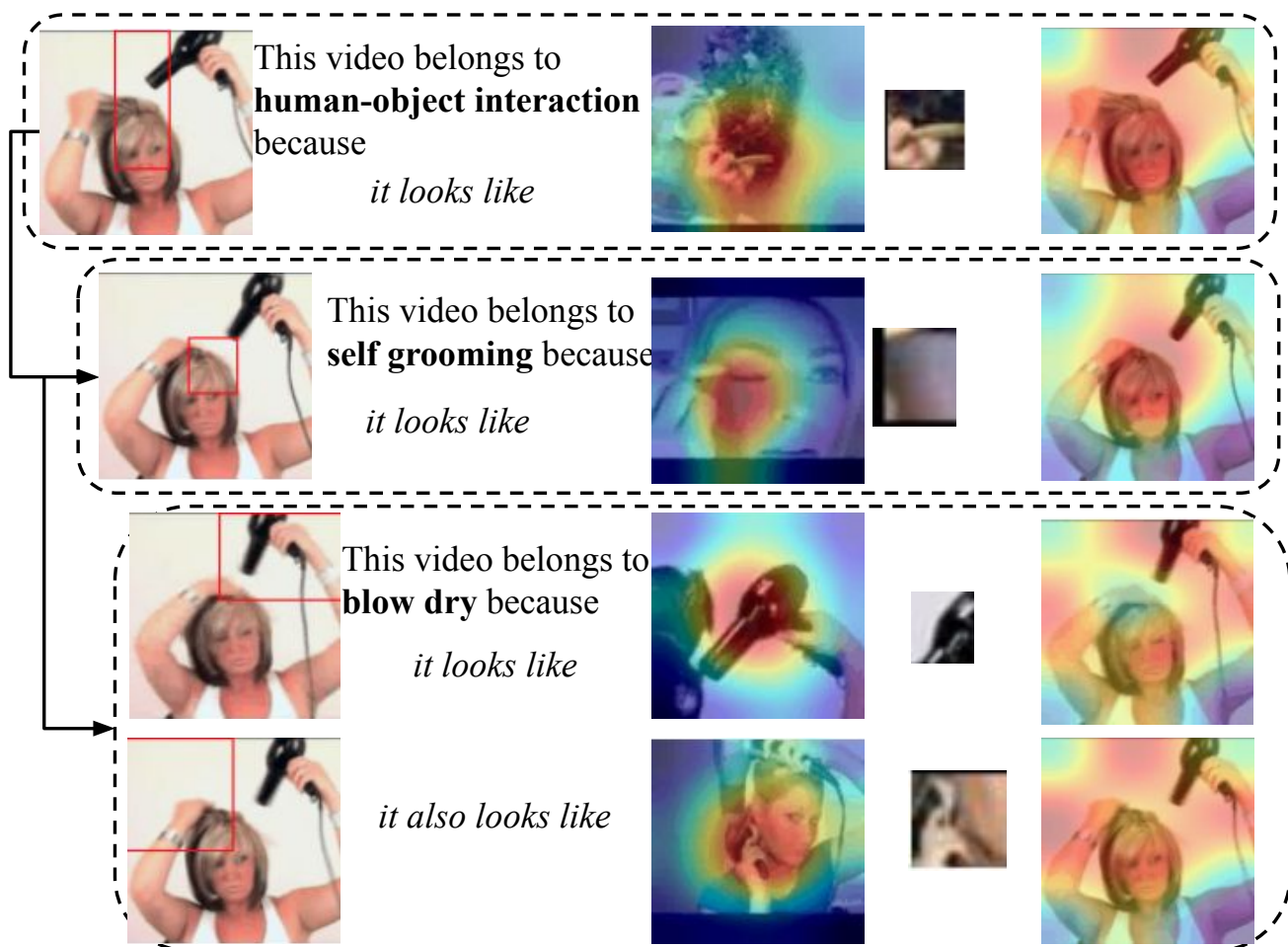
9. Qualitative Results

Figure 8, 9 and 10 show the quantitative results for our multi-level explanations, while Figure 12 and 11 show the effectiveness of our method in case of failure.



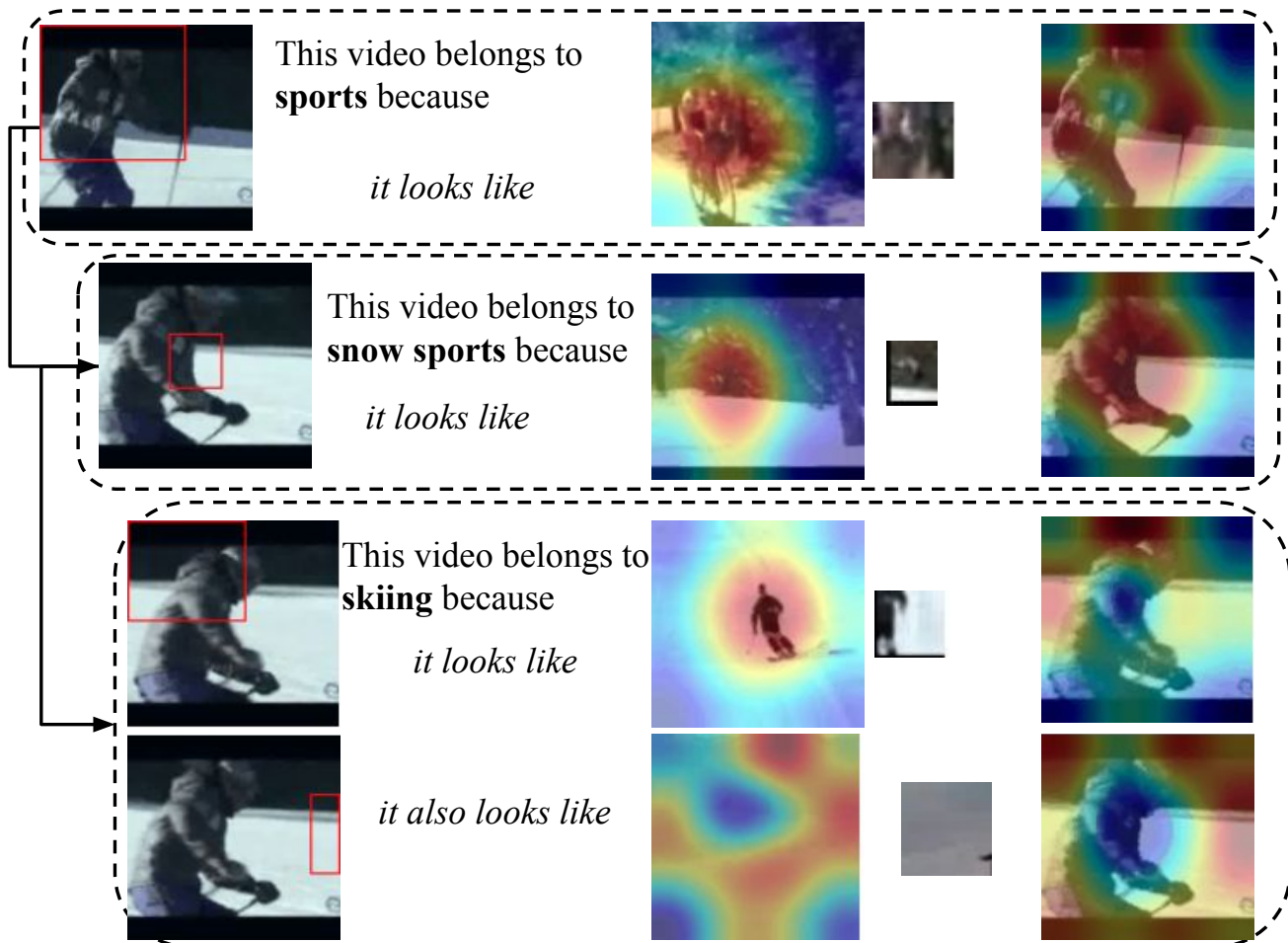
Leftmost: Parts in the original video that are highly activated by the prototype. *Second column:* Training videos where prototypes come from. *Third column:* Prototypes. *Rightmost:* Saliency map in the original video that are highly activated by the prototype.

Figure 8. **Multi-level Explanations.** Schematic representation of the hierarchical prototype-based reasoning process of our proposed Hierarchical ProtoPNet.



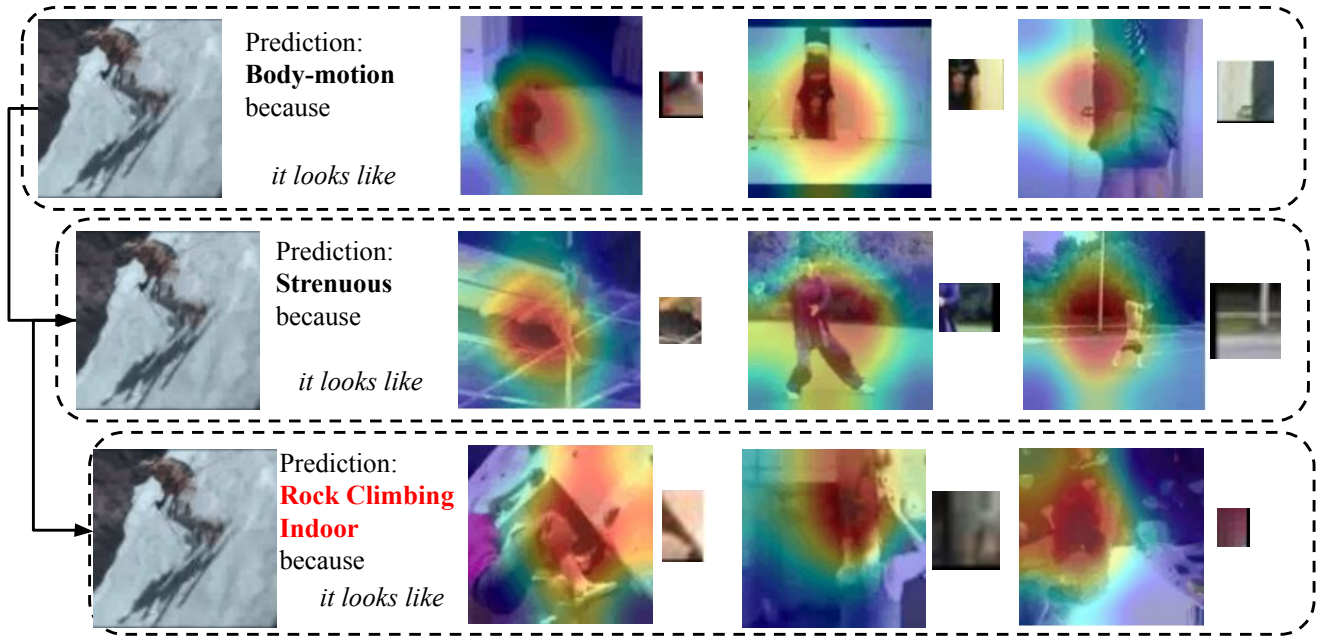
Leftmost: Parts in the original video that are highly activated by the prototype. *Second column:* Training videos where prototypes come from. *Third column:* Prototypes. *Rightmost:* Saliency map in the original video that are highly activated by the prototype.

Figure 9. **Multi-level Explanations.** Schematic representation of the hierarchical prototype-based reasoning process of our proposed Hierarchical ProtoPNet.



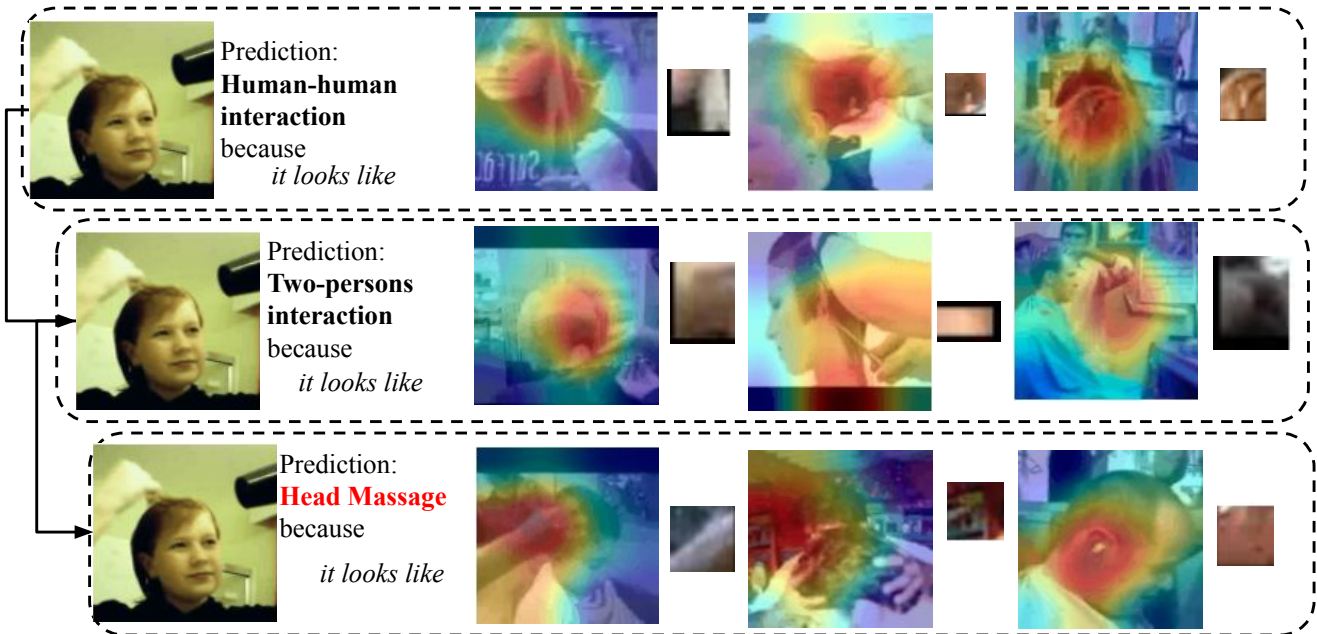
Leftmost: Parts in the original video that are highly activated by the prototype. *Second column:* Training videos where prototypes come from. *Third column:* Prototypes. *Rightmost:* Saliency map in the original video that are highly activated by the prototype.

Figure 10. **Multi-level Explanations.** Schematic representation of the hierarchical prototype-based reasoning process of our proposed Hierarchical ProtoPNet.



Leftmost: Original video. *Second column:* Three different training videos where prototypes come from. *Third column:* Prototypes.

Figure 11. **Effectiveness in case of failure.** Our multi-level explanations provide useful information even in the case of misclassification through the prototypes learned for parent and grandparent classes.



Leftmost: Original video. *Second column:* Three different training videos where prototypes come from. *Third column:* Prototypes.

Figure 12. **Effectiveness in case of failure.** Our multi-level explanations provide useful information even in the case of misclassification through the prototypes learned for parent and grandparent classes.